ELSEVIER

Organic Electronics 2 (2001) 75–82

Organic Electronics

www.elsevier.com/locate/orgel

STM investigation of vapor-deposition polymerization

S.F. Alvarado [a,*], W. Rieß [a], M. Jandke [b], P. Strohriegl [b]

[a] *Zurich Research Laboratory, IBM Research, Säumerstrasse 4, 8803 Rüschlikon, Switzerland*
[b] *Macromolecular Chemistry I, University of Bayreuth, 95440 Bayreuth, Germany*

Received 28 January 2001; received in revised form 9 February 2001; accepted 16 February 2001

Abstract

We present a study of vapor-deposition polymerization (VDP) to produce thin layers of poly(phenylquinoxaline) (PPQ), a material that can be used as an electron-transport layer in multilayer organic electroluminescent devices. The polymer is prepared by the thermally-induced polycondensation reaction of 1,3-bis(phenylglyoxaloyl)benzene and 3,3′-diaminobenzidine. The two monomers are deposited by evaporation onto an atomically clean Au(111) surface under ultrahigh-vacuum conditions. Polymer formation is monitored in situ by scanning tunneling microscopy. Photoluminscence (PL) spectroscopy measurements, performed in situ, reveal that the PL spectrum of the VDP product corresponds to a reference spectrum for solution-synthesized PPQ. For monolayer coverage, polymer clusters are formed with the chains oriented parallel to each other. STM images suggest that the VDP-prepared films can be much smoother and more uniform than films deposited by spin coating.

PACS: 81.15.Gh; 81.40.Tv; 73.61.Ph; 61.16.Ch
Keywords: STM; Vapor-deposition polymerization; Poly(phenylquinoxaline)

1. Introduction

Polycondensation is a large-scale industrial process used to produce millions of tons of commodity plastics such as poly(ethyleneterephthalate) (PET) and Nylon every year. The condensation of two different monomers each having two functional groups is usually carried out in the melt or, in fewer cases, in solution. Up to now, gas-phase processes have only seldom been used in polycondensations [1].

For some advanced applications, e.g. for optoelectronic devices such as organic light-emitting diodes (OLEDs), ultrathin polymer films with a thickness of 100 nm or less are required. Such films are usually made from polymer solutions by spin coating. An alternative approach to ultrathin organic layers is the use of low-molar-mass compounds which are thermally evaporated in high vacuum.

Vapor-deposition polymerization (VDP) is a gas-phase process that combines the characteristics of both processes. The principles of VDP are shown in Fig. 1. The evaporation process is carried out in a high-vacuum chamber. The two different monomers are heated in two separate crucibles, evaporated and then deposited simultaneously onto a common substrate. This coevaporation

* Corresponding author. Tel.: +41-1-724-8216; fax: +41-1-724-8958.
E-mail address: alv@zurich.ibm.com (S.F. Alvarado).

1566-1199/01/$ - see front matter
PII: S1566-1199(01)00012-X

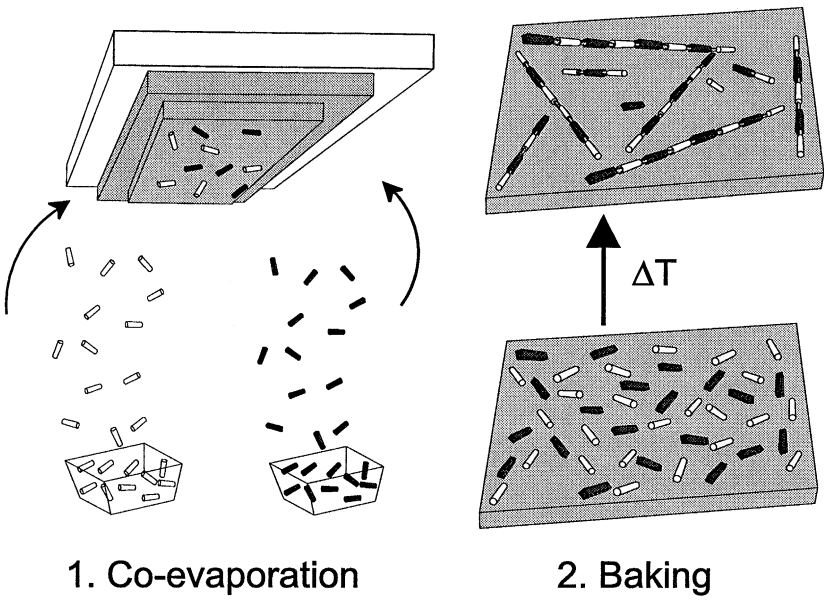

Fig. 1. Principle of vapor-deposition polymerization.

process is usually followed by a thermal treatment (baking step) in which a polymer is formed by a condensation reaction between the two monomers.

The solvent-free method guarantees clean and well-defined processing conditions. The coevaporation process offers access to insoluble or infusible polymers, which cannot be prepared from solution or melt. An in situ thickness control of the growing layer is possible, providing the option of preparing even thinner films than those that can be obtained by solution techniques such as spin coating. Thus vapor-deposition polymerization has become an interesting procedure for the preparation of thin dielectrics [2,3]. Recently first OLEDs using organic layers prepared by a variety of VDP methods have been described [4–8]. We have prepared thin layers of poly(phenylquinoxalines) (PPQs) serving as electron transporter in two-layer OLEDs [9]. Electron-deficient phenylquinoxalines are known to exhibit excellent properties regarding electron transport because of their high mobilities [10]. Their low-lying lowest unoccupied molecular orbital (LUMO) levels facilitate electron injection from various metal electrodes [11–14].

Here we present the first study in which polymer formation and polymer chain ordering of thin films produced by VDP were monitored directly in situ by means of scanning tunnelling microscopy (STM) and by photoluminescence (PL) spectroscopy. The entire experiment was carried out under ultrahigh-vacuum (UHV) conditions.

2. Experimental details

We used the two monomers 1,3-bis(phenylglyoxaloyl)benzene (tetraketone) and 3,3-diaminobenzidine (tetraamine). The tetraamine was purchased from Aldrich, whereas the tetraketone was prepared as described in [11]. Both monomers were carefully purified by repeated sublimating prior to use. The chemical structures of the tetraketone, the tetraamine and the polycondensation reaction are shown in Fig. 2. In the course of the polycondensation reaction four moles of water are split off.

The experiments were performed in a multichamber system under UHV conditions and with the base pressure in the lower 10^{-10} mbar region. Fig. 3 shows a schematic representation of the

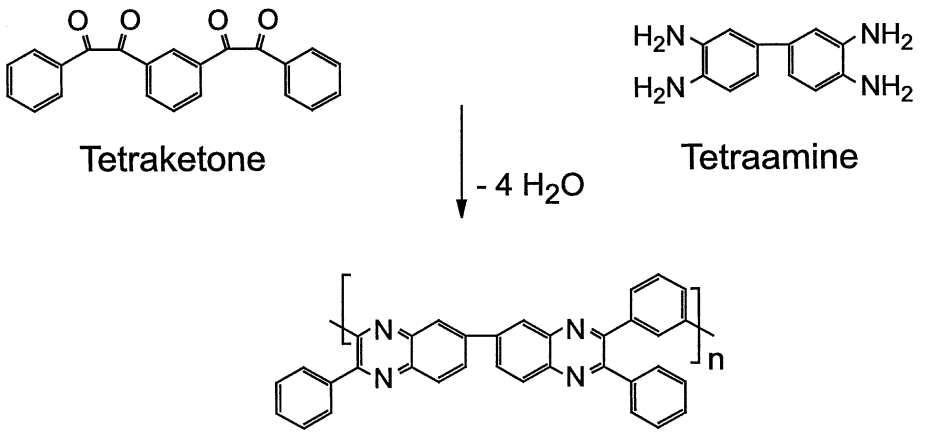

Fig. 2. Polycondensation reaction of 1,3-bis(phenylglyoxaloyl)beneze (tetraketone) and 3,3′-diaminobenzidine (tetraamine) to a poly(phenylquinoxaline) polymer.

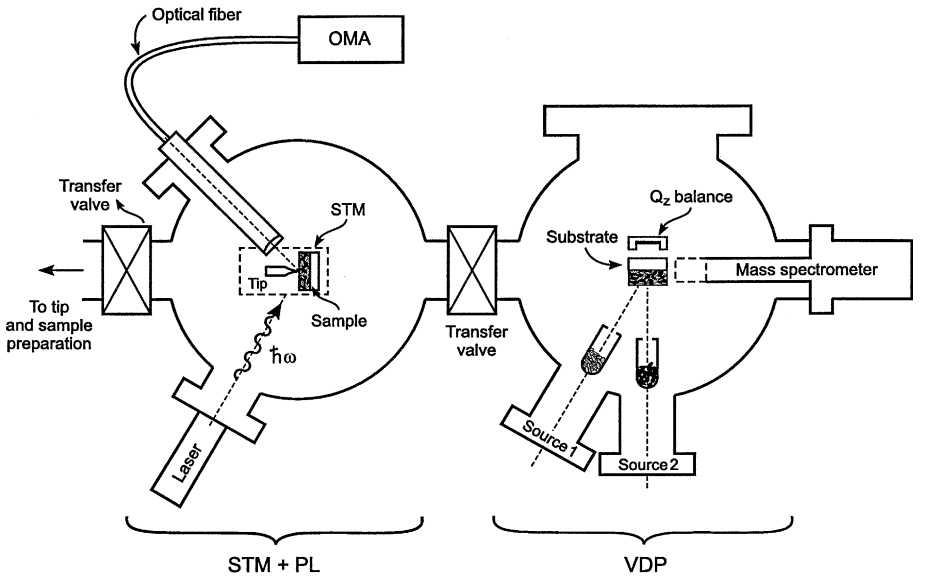

Fig. 3. Schematic of the UHV system consisting of an OMBE chamber, an STM/PL chamber, a tip and, not shown, a sample-preparation chamber and a load lock for introducing samples and tips. Samples can be moved between the various chambers without exposure to ambient conditions.

system. The organic molecular-beam evaporation chamber (OMBE) allows the simultaneous evaporation of both monomers onto a temperature-controlled substrate.

Each of the monomers is filled into a separate temperature-controlled effusion cell. Film-thickness monitoring is done by a quartz microbalance, whereas water eliminated during polycondensation is monitored by mass spectrometry. Prior to the VDP experiments the filled effusion cells as well as the substrates were thoroughly outgassed to minimize emission of residual gases and water molecules. An Au(111) single-crystal substrate was used. The substrate was cleaned by Ne-ion bombardment (800 eV) and annealed at 500°C. This leads to atomically clean substrate surfaces with

atomically flat terraces a few 100 nm in lateral extension, which exhibited the typical herringbone reconstruction [15]. The OMBE chamber is connected to a UHV chamber equipped with an STM (see Fig. 3). Samples can be transferred between the chambers without exposure to ambient conditions. For the STM work Pt/Ir tips are used. In addition, characterization of the samples can be done by PL while the samples are in the STM chamber. The thickness of the PPQ polymer films was estimated by using the STM to measure the tip-height difference at low tunneling voltage bias, $V_T = 0.1$ V, where the tip images the substrate, and at high V_T (typically 2–3 V), where the tip images the surface of the thin polymer film. For details of this technique see [16,17].

3. Results and discussion

Our aim was to monitor polymer formation during polycondensation by means of STM. For this purpose we first deposited a thin film, half a monolayer (ML) thick, of the tetraketone monomer on a Au(111) substrate at room temperature. Fig. 4 shows an STM image in two different magnifications. Fig. 4(a) shows that the tetraketone accumulates by forming clusters at the corners of the atomic terraces on the gold surface. The clusters have an average diameter of 10 nm and a height of about 2.5 nm. This demonstrates the high mobility of the tetraketone on the gold surface, which is a prerequisite for polycondensation. An STM image with higher magnification (Fig. 4(b)) shows ordered molecular features, indicating that the clusters consist of cyrstallized tetraketon molecules. The periodicity of the molecular features (≈5 Å) in the image corresponds approximately to the distance between two phenyl rings in the tetraketone molecule [18].

The next step of the experiment was to deposit ≈0.5 ML of diaminobenzidine on this tetraketone-covered substrate. The STM image (Fig. 5) shows that the benzidine molecules form larger clusters. The smaller tetraketone clusters, however, are no longer visible, suggesting that they have become engulfed by the tetraamine. Note that cyrstalline order can no longer be discerned in the STM images.

Then the substrate with the two monomers was heated to 280°C. From studies using differential scanning calorimetry we know that the high temperature is necessary to complete the polycondensation reaction. Fig. 6 shows STM images of the product of the reaction.

For this low coverage (0.5 ML tetraketone + 0.5 ML tetraamine), the STM reveals that the reaction product forms isolated clusters, a few

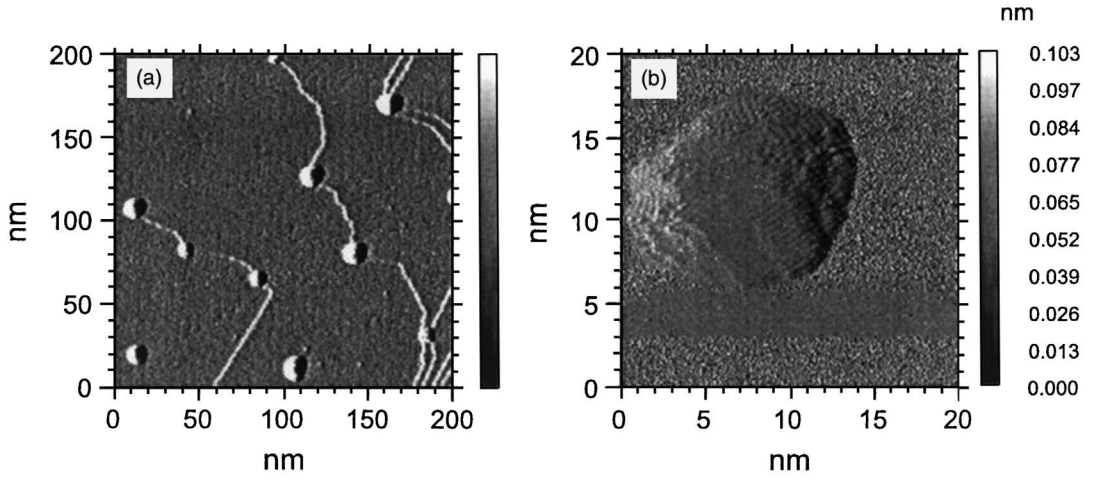

Fig. 4. STM images showing Au(1 1 1) substrate after deposition of half a mono-layer of tetraketone in two different magnifications. The tetraketone forms crystalline clusters at the terrace corners of the substrate.

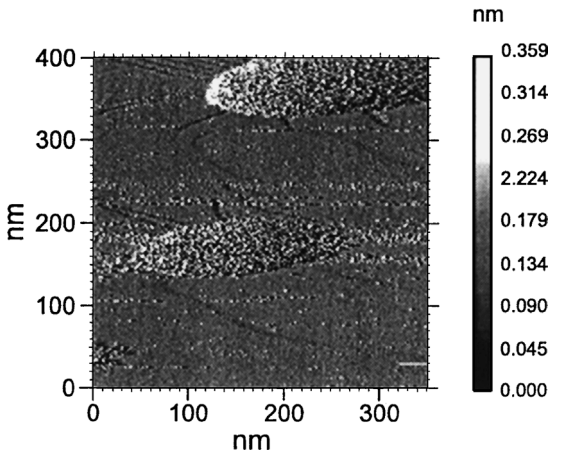

Fig. 5. STM image of the tetraketone-covered substrate (see Fig. 4) after deposition of half a monolayer of tetraamine: the tetraketone clusters have been engulfed by the tetraamine, resulting in extended clusters exhibiting no crystalline order.

100 nm in lateral extension, each consisting of arrays of polymer chains tightly bundled together and that the polymer chains are oriented parallel to each other. In some cases monolayer polymer sheets seem to emanate from the base of the clusters. Fig. 6 shows an image of such a polymer sheet. In this case it is possible to obtain molecular resolution as the polymer chains are fixed because of the interaction with the substrate. STM images collected from different locations on the film indicate that the polymer chains are oriented along preferred directions. These preliminary results suggest that substrate topographic features, such as steps, direct chain packing. The spacing of the bright spots in the image suggests that they correspond to repeat units in the polymer chain. A possible model of the arrangement of the chains is shown in Fig. 7(b). A rough estimate of the length of the polymer repeat unit can be obtained from a MOPAC calculation (MSI Cerius 3.5) for a dimer of the PPQ structure (Fig. 7(a)). On the clusters it was not possible to observe molecular details with such high resolution. This is may be due to the lack of rigidity of the bulk polymeric material, which tends to yield and move in response to the forces exerted by the tip of the STM.

The evolution of water during the polymerization step was monitored by mass spectrometry. Given the detection limit of the mass spectrometer used, a 20-nm-thick sample (10 nm tetraketone + 10 nm tetraamine, nominal thickness) was prepared by coevaporation of the two monomers on the clean Au(111) substrate at room temperature. The evolution of water during the heat treatment is shown in Fig. 8. It can clearly be seen that water begins to split off at ≈100°C, a temperature corresponding to the melting point of the tetraketone. The maximum amount of water evolves at ≈185°C, close to the melting point of tetraamine

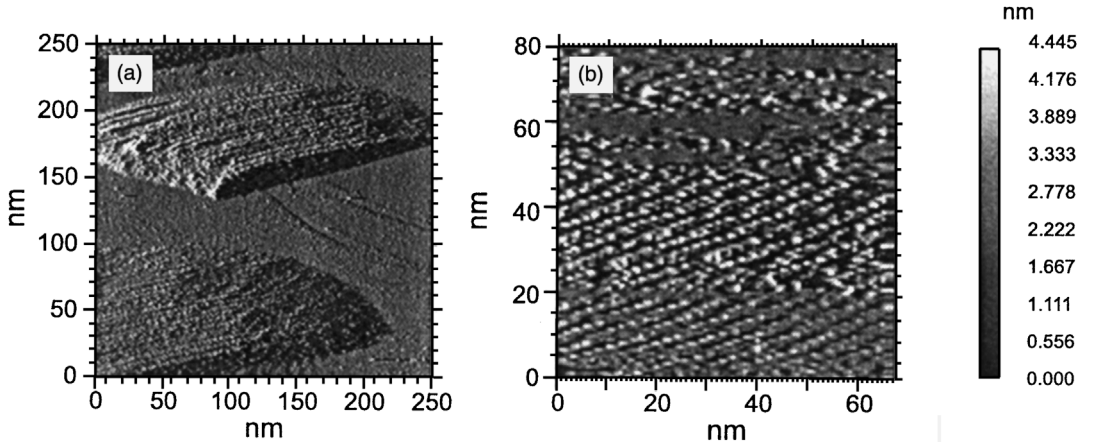

Fig. 6. STM images of the reaction product of 0.5 ML tetraketone and 0.5 ML tetraamine, see Figs. 4 and 5, obtained after heating to 280°C.

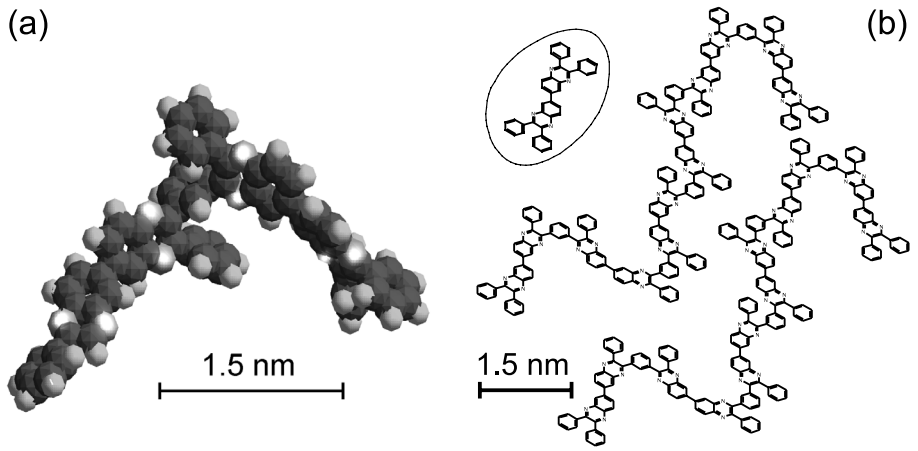

Fig. 7. (a) MOPAC calculations for a phenylquinoxaline dimer. (b) Possible chain conformations for the observed orientation of PPQ in Fig. 6.

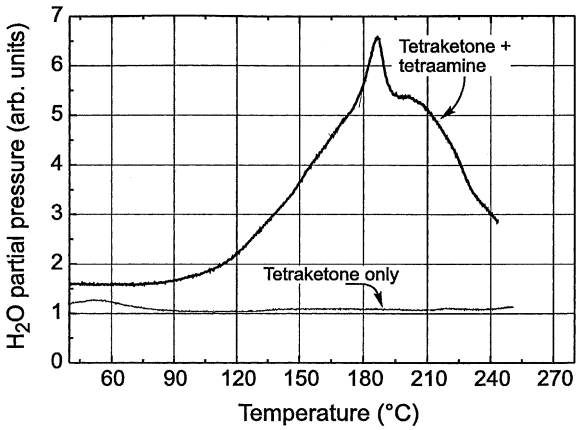

Fig. 8. In situ mass-spectroscopic investigation of the water formed during baking process; upper curve: tetraketone and tetraamine film (20 nm); lower curve: tetraketone film (20 nm).

(175–177°C), because of the enhanced diffusion of the two monomers in the liquid phase. Thereafter the evolution of water decreases with increasing temperature as the reaction comes to an end owing to reactant depletion. We have also observed this behavior in model differential scanning calorimetry studies of 1:1 mixtures of tetraketone and tetraamine monomers. The amount of water decreases with increasing temperature and finally reaches the background level. The lower curve in Fig. 8 shows the reference curve measured on a substrate covered only with tetraketone monomer. After thermal treatment of the 20-nm-thick tetraketone + tetraamine film, the PPQ layer had an average thickness of about 4 nm, as determined with the STM by means of tip-height versus tunnel voltage measurements [16]. This reduction in thickness is partly due to reevaporation of unreacted tetraketone and tetraamine molecules from the substrate. The determination of the exact material attrition for given thermal treatment parameters requires more precise studies at different heating rates, curing temperatures and times. PL spectroscopy measurements, performed in situ, reveal that the PL spectrum of the VDP product corresponds well to the reference spectrum for solution-polymerized PPQ ($M_w = 15,000$ g/mol [11]), see Fig. 9. The VDP-PPQ spectrum shows a blue shift of $\approx$11 nm, which could be explained by the different morphologies of the well ordered PPQ obtained by VDP and the solution cast PPQ reference sample. STM images suggest that the films prepared by VDP are much smoother and more uniform than polymer thin films, e.g. poly(*p*-phenylenevynelene) and its derivatives, that we have deposited by spin coating. The PPQ film exhibits no pinholes. An STM trace demonstrating the uniformity of the PPQ thin film is shown in Fig. 10. In this particular region of the film, the thickness is 3.3 ± 0.6 nm. The fluctuations of

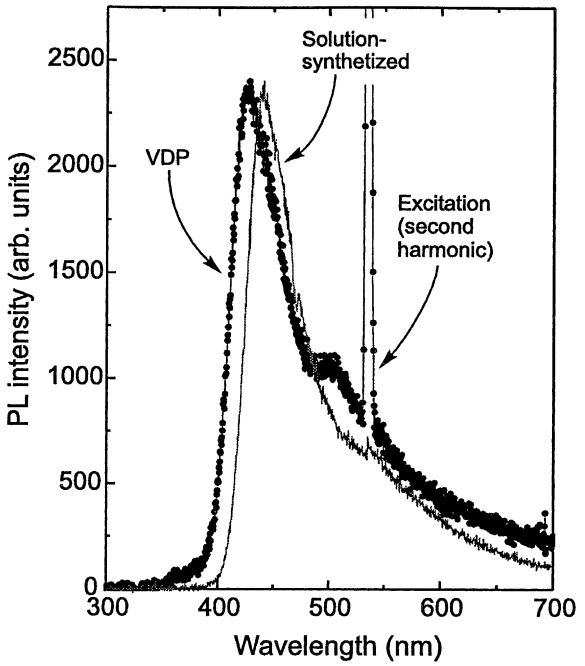

Fig. 9. Photoluminescence spectrum of a 3.3-nm-thick PPQ thin film prepared by UHV VDP (●). A reference spectrum obtained on solution-synthesized PPQ is also shown (—).

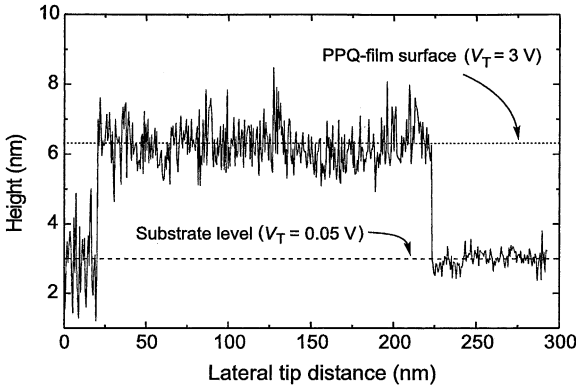

Fig. 10. STM trace collected at low and high tunneling voltage biases (lower and higher levels respectively), allowing an estimate of the thickness and uniformity of the VDP-grown PPQ film. The mean film thickness is 3.3 ± 0.6 nm over lateral distances of several 100 nm.

0.6 nm correspond approximately to the polymer chain thickness.

In addition, preliminary measurements of the band gap for charge-carrier injection were done using STM $z(V)$ spectroscopy [16,17]. The observed band gap of about 3.1 eV differs from the optical band gap derived from absorption measurements, 2.96 eV. The energy difference can be attributed to the exciton binding energy.

4. Conclusions

We have prepared ultrathin films of poly(phenylquinoxaline) by VDP. All reaction steps, including the evaporation of the two monomers, the thermal treatment and the STM characterization, have been carried out under UHV conditions, leading to clean materials and interfaces. The polycondensation process could be monitored by in situ mass spectroscopy and photoluminescence. Evaporation of the two monomers leads to the formation of intermixed clusters that favor the condensation reaction. For monolayer coverage, the clusters are isolated and the substrate is not fully wetted. For a sample having an initial thickness of unreacted material of ≈20 nm, however, the polymer film obtained, which is only a few nanometer thick, exhibits no pin holes and has a smoothness that indicates a superior quality compared to that of films produced by standard solution-deposition techniques such as spin coating. We provide direct evidence that the thermally activated reaction of the mixed clusters gives rise to arrays of polymer chains ordered parallel to each other. This experiment shows for the first time that using STM it is possible to visualize the morphological changes during polymer formation.

Acknowledgements

This work was performed within the Training and Mobility of Researchers Network EURO-LED, contract no. ERB-FMRX-CT97-0106.

References

[1] J.R. Salem, F.O. Sequeda, J. Duran, W.Y. Lee, R.M. Yang, J. Vac. Sci. Technol. A 4/3 (1986) 369.
[2] Y. Takahashi, M. Iijima, Y. Oishi, M. Kakimoto, Y. Imai, Macromolecules 24 (1991) 3543.
[3] M. Iijima, Y. Takahashi, Macromolecules 22 (1989) 2944.

[4] E.G. Staring, D. Braun, G.L. Rikken, R.J. Demandt, Y.A. Kessener, M. Bouwmans, D. Broer, Synth. Met. 67 (1994) 71.
[5] O. Schaefer, A. Greiner, J. Pommerehne, W. Guss, H. Vestweber, H. Tak, H. Baessler, C. Schmidt, G. Luessem, B. Schartl, V. Stuempflen, J.H. Wendroff, S. Spiegel, C. Moeller, H.W. Spiess, Synth. Met. 82 (1996) 1.
[6] W. Fischer, F. Stelzer, F. Meghdadi, G. Leising, Synth. Met. 76 (1996) 201.
[7] H. Murata, S. Ukishima, H. Hirano, T. Yamanaka, Poly. Adv. Technol. 8 (1997) 459.
[8] M. Tamada, H. Koshikawa, F. Hosoi, T. Suwa, H. Usui, A. Kosaka, H. Sato, Polymer 40 (1999) 3061.
[9] M. Jandke, K. Kreger, P. Strohriegl, Synth. Met. 111–112 (2000) 221.
[10] M. Redecker, D.D.C. Bradley, M. Jandke, P. Strohriegl, Appl. Phys. Lett. 75 (1999) 109.
[11] M. Jandke, P. Strohriegl, S. Berleb, E. Werner, W. Bruetting, Macromolecules 31 (1998) 6434.
[12] H. Schuermann, N. Koch, P. Imperia, S. Schrader, M. Jandke, P. Strohriegl, B. Schulz, G. Leising, L. Brehmer, Synth. Met. 102 (1999) 1069.
[13] D. O'Brien, M.S. Weaver, D.G. Lidzey, D.D.C. Bradley, Appl. Phys. Lett. 69 (1996) 881.
[14] T. Yamamoto, K. Sugiyama, T. Kushida, T. Inoue, T. Kanbara, J. Am. Chem. Soc. 118 (1996) 3930.
[15] J.V. Barth, H. Burne, G. Ertl, R.J. Behm, Phys. Rev. B 42 (1990) 9307.
[16] S.F. Alvarado, P.F. Seidler, D.G. Lidzey, D.D.C. Bradely, Phys. Rev. Lett. 81 (1998) 1082.
[17] S.F. Alvarado, L. Rossi, P. Müller, P.F. Seidler, W. Riess, IBM J. Res. Develop. 45 (2001) 89.
[18] A. Syed, E.D. Stevens, Acta Cryst. C 40 (1984) 1271.